

Acknowledgements We are grateful to members of our laboratory and to K. Mitrophanous, J. M. Park and H. E. Kim for their critical reading of this manuscript and for discussion. This work was supported by the Korea Research Foundation and the BK21 Research Fellowship from the Ministry of Education and Human Resources Development of Korea.

Competing interests statement The authors declare that they have no competing financial interests.

Correspondence and requests for materials should be addressed to V.N.K. (narrykim@snu.ac.kr).

A structural state of the myosin V motor without bound nucleotide

Pierre-Damien Coureux¹, Amber L. Wells², Julie Ménétreay¹, Christopher M. Yengo², Carl A. Morris², H. Lee Sweeney² & Anne Houdusse¹

¹Structural Motility, Institut Curie CNRS, UMR144, 26 rue d'Ulm, 75248 Paris cedex 05, France

²Department of Physiology, University of Pennsylvania School of Medicine, 3700 Hamilton Walk, Philadelphia, Pennsylvania 19104-6085, USA

The myosin superfamily of molecular motors use ATP hydrolysis and actin-activated product release to produce directed movement and force¹. Although this is generally thought to involve movement of a mechanical lever arm attached to a motor core^{1,2}, the structural details of the rearrangement in myosin that drive the lever arm motion on actin attachment are unknown. Motivated by kinetic evidence that the processive unconventional myosin, myosin V, populates a unique state in the absence of nucleotide and actin, we obtained a 2.0 Å structure of a myosin V fragment. Here we reveal a conformation of myosin without bound nucleotide. The nucleotide-binding site has adopted new conformations of the nucleotide-binding elements that reduce the affinity for the nucleotide. The major cleft in the molecule has closed, and the lever arm has assumed a position consistent with that in an actomyosin rigor complex. These changes have been accomplished by relative movements of the subdomains of the molecule, and reveal elements of the structural communication between the actin-binding interface and nucleotide-binding site of myosin that underlie the mechanism of chemo-mechanical transduction.

Myosin V is a myosin motor that has a number of structural and kinetic features that allow it to act as a two-headed processive motor protein³. The most notable feature is its long tandem repeat of six calmodulin/light-chain-binding sites, which form a long 'lever arm' that allows myosin V to take multiple 36-nm steps along an actin filament without detachment (that is, processive movement)^{3,4}. This allows the molecule to function as a vesicle transporter⁵. To achieve processive movement, the rates of key kinetic steps of myosin V are very different from myosin II, which results in each head spending most of its ATPase cycle strongly bound to actin⁶.

The current view of how myosin couples ATP hydrolysis and actin binding to movement is known as the lever arm hypothesis^{1,2}. In essence the proposed mechanism is that nucleotide binding, hydrolysis and product release are all coupled to small movements within the myosin motor core. These movements are amplified and transmitted by a region that has been termed the 'converter'^{7,8} to a lever arm consisting of a light-chain-binding helix and associated light chains. The lever arm further amplifies the motions of the converter into large directed movements⁷⁻⁹. In the absence of actin, ATP hydrolysis occurs, but product release is slow, thus trapping the

lever arm in a primed or pre-power-stroke position. Binding to actin causes release of products, movement of the lever arm, and force generation concomitant with formation of strong binding between myosin and actin (see Supplementary Fig. 1).

Although there is growing evidence for this general scheme¹, the proposed structural details of the motor domain changes are based entirely on high-resolution structures of myosin II in states that bind weakly to actin, and thus do not represent force-generating states². Crystals with either vanadate or AlF₄ plus MgADP reveal a state (the 'transition' state) that probably mimics the pre-power-stroke state of myosin compatible with ATP hydrolysis, and before actin binding^{7,10,11}. The 'near-rigor' state, which has been seen with MgADP, MgATP, ATP analogues or no nucleotide in the active site^{12,13}, has been proposed to reveal the position of the myosin lever arm at the end of the power stroke on release of MgADP (an actomyosin state known as rigor). However, it cannot truly represent such a state as there is considerable kinetic evidence that demonstrates that the near-rigor conformation of myosin II cannot bind strongly to actin without significant structural rearrangements^{2,14}. Thus current crystal structures of myosin II offer no explanation of how actin-induced product release increases the affinity of myosin for actin, and how ATP dissociates the actin-myosin nucleotide-free (rigor) complex after release of phosphate and MgADP.

As previously noted⁶ (see also Supplementary Fig. 2), in the absence of nucleotide an expressed truncated form (truncated after the first calmodulin-binding domain) of myosin V with a bound essential light chain (LC1-sa with the extended amino terminus removed¹⁵) binds rapidly to actin in a concentration-dependent manner, is not temperature dependent, and does not saturate over the actin concentrations examined. The rate of skeletal myosin II actin binding is highly temperature dependent and saturates at a moderate rate and actin concentration¹⁶. This indicates that in the absence of nucleotide and actin, myosin II—which mostly populates the near-rigor conformational state—is in a very different conformation from that in the rigor complex that forms after adding actin. On the other hand, the kinetics of myosin V binding appear to be diffusion limited⁶, implying that myosin V in the absence of nucleotide and actin is in a state that is nearly equivalent to the rigor state formed on the addition of actin.

Crystals of this nucleotide-free myosin V construct diffracted to 2.0 Å. The refined structure is unlike that of any of the myosin structures to date. However, as compared to the near-rigor or pre-power-stroke structures, the lever arm is in a position that is similar to that of the near-rigor state (see Supplementary Fig. 3).

Figure 1a demonstrates that there have been movements of the previously defined⁸ subdomains of the myosin motor that allow a different actin interface, closure of a major cleft (50-kDa cleft) in the molecule, and weakening of nucleotide binding. These subdomains of the motor, which have been proposed to move as units connected by flexible connectors or 'joints', are the N-terminal, upper 50-kDa and lower 50-kDa subdomains, and the converter (to which the lever arm is attached). This structure reveals new conformations of the previously defined connectors⁸ (switch II, relay and SH1 helix) as well as revealing the importance of a fourth connector (previously termed the 'strut'¹⁷), which links the lower and upper 50-kDa subdomains near the actin interface. Precise interactions mediated by these connectors, that are different for each myosin state, allow stabilization of the unique subdomain positions in each state. In our new state, for the first time in any myosin structure, there is a significant movement (25° rotation) of the upper 50-kDa subdomain relative to the N-terminal subdomain. As discussed below, this movement is critical for both rearrangement of the nucleotide-binding pocket and closure of the internal cleft between the two 50-kDa subdomains.

On the basis of attempts to dock the initial and subsequent high-resolution structures of myosin II into lower-resolution cryo-

electron microscopy reconstructions of the actin–myosin complex, it has been predicted that the 50-kDa cleft in the myosin molecule would have to close in order to create the rigor interaction^{18,19}. In our new structure, the actin interface is quite different from those of the near-rigor or transition states, owing to a relative rotation and translation of the upper and lower 50-kDa subdomains resulting in closure of the cleft (Fig. 1a) both near the actin- and nucleotide-binding sites. The closure near the actin-binding site requires a conformational change in a connector between the upper and lower 50-kDa subdomains (the strut) that allows it to interact specifically with both subdomains (Fig. 1b). Changes in the strut also allow a large number of direct interactions between the upper and lower 50-kDa subdomains, including a number of van de Waals interactions and specific side-chain interactions. Mutagenesis studies have demonstrated that alterations in the length of the strut prevent strong binding to actin¹⁷.

Previous evidence for some degree of cleft closure on formation of the actin–myosin rigor complex includes a fluorescence change of an engineered tryptophan (F425W) in the upper 50-kDa sub-

main of smooth muscle myosin II²⁰. In our structure the corresponding residue, N398, forms hydrogen bonds with residues of both the lower 50-kDa subdomain and the strut (Fig. 1b). It is also known that formation of the actin–myosin rigor complex requires a conformational change in myosin II that results in a net exclusion of water molecules from the motor¹⁴. The cleft closure seen in our structure results in exclusion of a considerable amount of water from the molecule, obliterating the aqueous tunnel seen in the near-rigor structure (Fig. 1a).

Another major prediction based on the first myosin II structure was that there would be an opening of the nucleotide pocket triggered by cleft closure (actin binding) to release MgADP¹². However, the elements that coordinate the nucleotide (P loop, switch I) have not been observed to move significantly, even in myosin structures to date that do not have bound nucleotide¹³. In our myosin V structure, the possibility of high-affinity nucleotide binding has been eliminated in a series of unexpected structural rearrangements, rather than a simple opening of the pocket. The P loop and switch I have moved approximately 6.5 Å apart, destroying

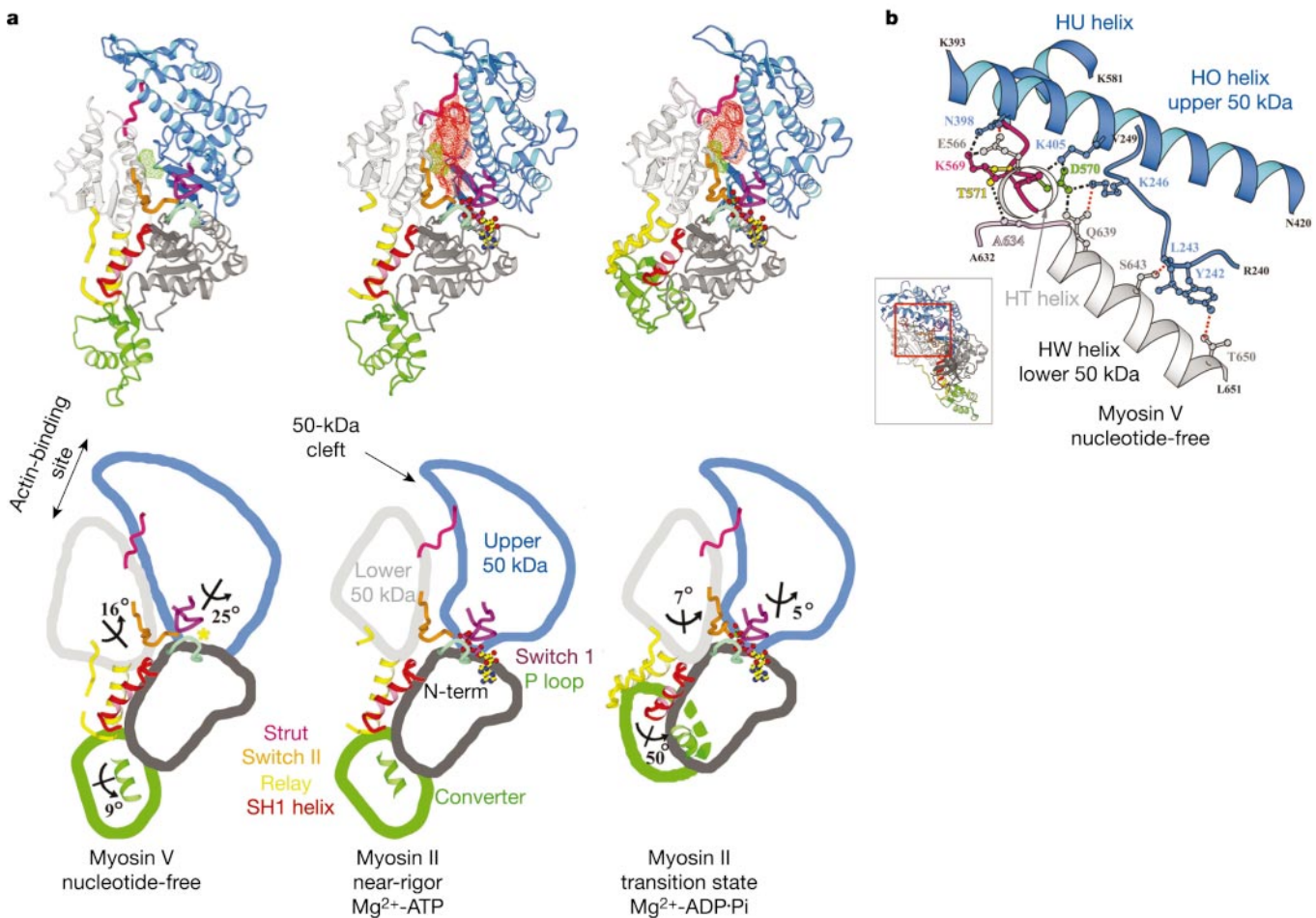


Figure 1 Positions of subdomains and connectors in the three myosin states and closure of the 50-kDa cleft. **a**, A comparison of the myosin V motor domain to the *Dictyostelium* myosin II in the near-rigor and transition states shows the different positions of the subdomains, nucleotide-binding elements and connectors in each state. The structures have been superimposed on the N-terminal subdomains. Relative to this subdomain, the rotation necessary to move from the myosin V state to the near-rigor state is indicated for each subdomain of myosin V; similarly, the rotation necessary to move from the near-rigor to the transition state is indicated on the subdomains of the transition-state structure. Contours of the solvent-accessible cavities for the near-rigor ($1,735 \pm 173 \text{ \AA}^3$) and

transition states ($795 \pm 140 \text{ \AA}^3$) are shown with a red contour, whereas the green contour ($73 \pm 27 \text{ \AA}^3$) depicted in all structures represents an internal cavity of myosin V. Pi, inorganic phosphate. **b**, Shown are specific hydrogen bonds involving the strut that result in cleft closure near the actin interface. Of note is the interaction of D570 with K405 and K246, which are residues conserved in all myosins. However, a number of residues involved in cleft closure in our structure (such as T571, K569, N398) are not absolutely conserved in the myosin superfamily. Variability in cleft interactions could alter the kinetics of cleft closure, and thus the rate of the weak-to-strong binding to actin.

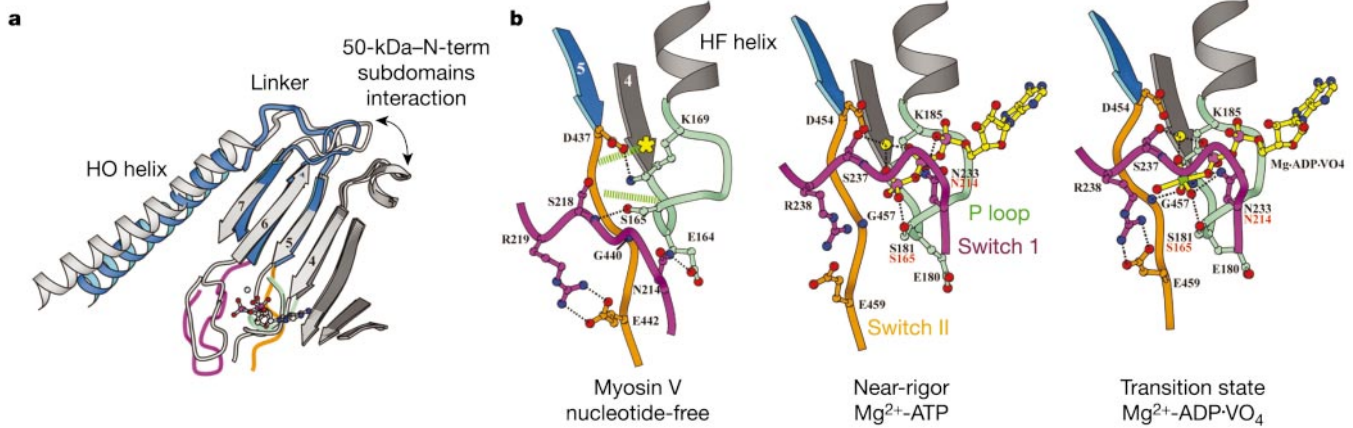


Figure 2 Nucleotide-binding site and distortion of the β -sheet at the interface of the N-terminal and upper 50-kDa subdomains. **a**, Shown is an overlay of the β -sheet (N-terminal subdomain superimposed) between myosin V in blue and near rigor (*Dictyostelium* myosin II) in grey. Note that strands 5–7, which belong to the upper 50-kDa subdomain are distorted to allow the upper 50-kDa rotation that removes switch I from the nucleotide-binding site. **b**, The positions of the nucleotide-binding elements are shown for

three myosin states. The yellow asterisk in the myosin V structure marks the position of the Mg^{2+} in the other structures. In the transition state, switch II contributes to coordination of the γ -phosphate of the nucleotide, but it bends in myosin V in the opposite direction and forms direct interactions (broken green lines) with the fourth β -strand and the P loop of the N-terminal subdomain.

the ability to coordinate Mg^{2+} and the possibility of switch I interactions with nucleotide. A new conformation of switch II is stabilized by a number of new interactions (Fig. 2b). Note that the switch I conformation is not altered, but simply follows the movement of the upper 50-kDa subdomain relative to the P loop and N-terminal subdomain (Fig. 2a). The position of the P loop itself appears to provide steric hindrance to nucleotide entry (Fig. 2a). However, as its position in our structure is stabilized by weak

interactions, we would anticipate that in solution the P loop would rapidly explore other conformations and would not significantly hinder ATP binding.

A distortion of the seven-stranded β -sheet that couples the N-terminal and upper 50-kDa subdomains is essential to allow the large movement of the upper 50-kDa subdomain (including switch I). Although the amplitude of this distortion is large (Fig. 2a), the key interactions that maintain the sheet have not been altered

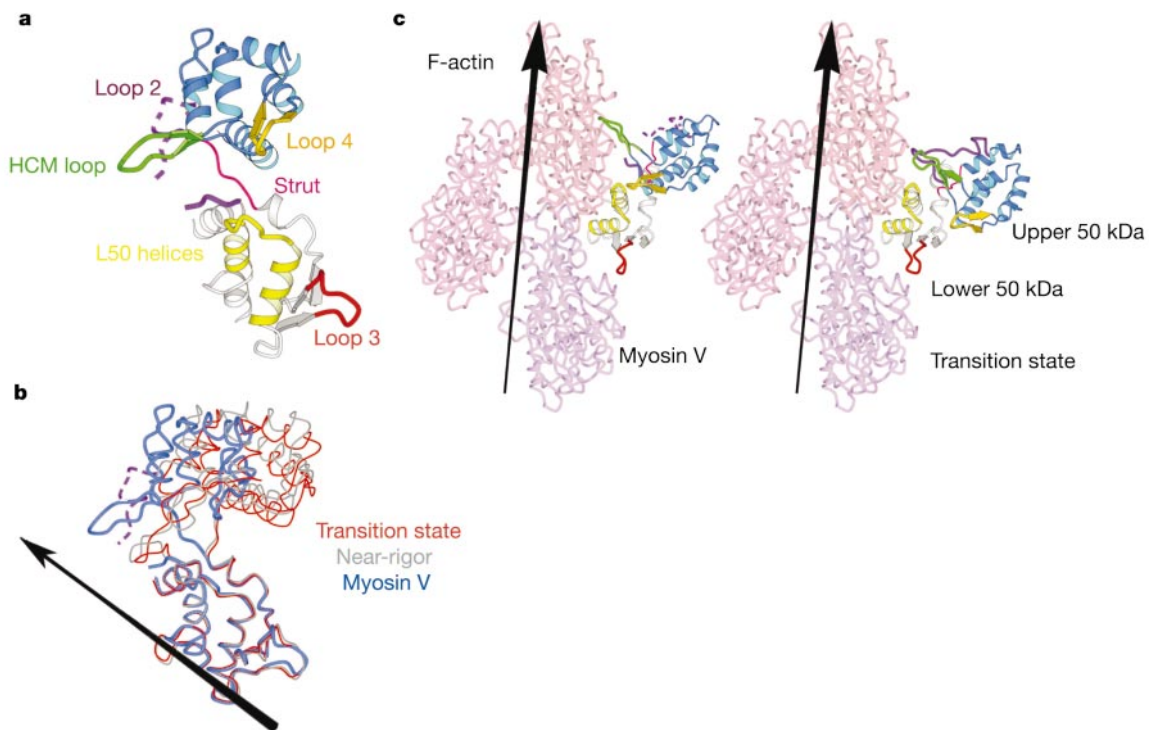


Figure 3 The actin–myosin interface. **a**, Myosin V as viewed from the actin side of the interface reveals the positioning of putative actin-binding elements. **b**, The same view of myosin V is overlaid on the lower 50-kDa subdomains of *Dictyostelium* myosin II structures. Note the conformational change in the strut and the obvious rotation of the upper 50-kDa subdomain towards the actin filament (represented by an arrow) in the

myosin V structure. **c**, The myosin V and transition state actin-binding elements are docked on an actin filament, maintaining the identical positioning of the lower 50-kDa subdomain in both cases. In myosin V, the HCM loop has been repositioned in such a way that it can directly contribute to actin binding.

(unlike what is observed for ARF proteins²¹). The distortion of strands 5–7 of the β -sheet allows switch I and II to follow the rotation of the upper 50-kDa subdomain, while maintaining the upper 50-kDa–N-terminal subdomain interactions on the opposite side of the sheet (Fig. 2a). (A similar β -sheet distortion has also been observed in a new structural state of *Dictyostelium* myosin II (F. J. Kull and D. J. Manstein, personal communication).) This distortion (that is, structural change that does not simply follow the subdomain movement) is greatest for strand 5. That strand connects on one side to switch II, and on the opposite side to a linker coming from the longest helix (HO) of the upper 50-kDa subdomain that begins at the actin interface (HCM loop²², see below). Through this helix, the linker can provide coupling between the β -sheet and the actin interface, and itself undergoes considerable distortion in our new state as compared with either of the weak binding states (transition or near-rigor states).

Switch II has an important role in the positioning of the subdomains that are critical for cleft closure and lever arm position in the new state. Notably, switch II promotes a different set of interactions between the subdomains in the transition state structure. This results in the partial cleft closure of the transition state, as compared to the near-rigor state, which traps the phosphate after ATP hydrolysis and results in repositioning of the lever arm in its pre-power-stroke conformation. However, the interactions that close the cleft in the transition state are not all maintained in our new state. Indeed, part of the region that is closed in the transition state opens to form a small internal cavity in the nucleotide-free structure (Fig. 1a).

If one assumes that the interface between the lower 50-kDa subdomain and actin is essentially the same in all myosin states, then our new structure would form a more extensive interface with actin because the upper 50-kDa subdomain has been moved close to the actin surface. In particular, the HCM loop—which is known to contribute hydrophobic interactions to create strong actin binding²²—and a previously uninvestigated loop (loop 4)¹¹ are now in position to make actin interactions (Fig. 3). Thus our new structure would be predicted to provide a much better fit to either a myosin II or myosin V rigor cryo-electron microscopy map near the actin interface than do any of the existing myosin II near-rigor structures.

On the basis of all of the structural and kinetic evidence described above, we propose that our myosin V structure is a rigor-like state. The positions of the switch elements and the β -sheet seen in our structure explain how cleft closure induced by actin binding results in the weakening of nucleotide affinity. If this rigor-like structure then rearranges to the conformation seen in the near-rigor state on introduction of ATP, it would explain how ATP binding to the actomyosin rigor complex weakens the affinity of myosin for actin. The sequence of events would be initial binding of the phosphates of ATP to the P loop, followed by an inward movement of switch I to coordinate the γ - and β -phosphates and the Mg^{2+} ion. This switch I movement would be mediated by rearrangement of the β -sheet, and accompanied by movement of switch II, and a reopening of the cleft. (The necessity of switch II movement in the transition from rigor to near-rigor is supported by a mutation of switch II (G440A) of myosin V that greatly slows ATP-induced dissociation from actin, while allowing ATP binding²³.) This would decrease the affinity of the myosin for actin, leading to dissociation of the myosin coincident with formation of the near-rigor state. This isomerization and dissociation occurs with minimal movement of the converter and lever arm. Thus ATP binding does not reverse the lever arm movement. Reversal or repriming occurs on isomerization from the near-rigor state to the transition state (while myosin is detached from actin), which immediately precedes ATP hydrolysis.

What cannot be deduced from the myosin V rigor structure are details of the myosin states between the initial weakly bound actin–myosin–ADP–Pi state and the actin–myosin rigor complex. In these

states, phosphate followed by MgADP is released from the myosin. The key interactions between actin and myosin that trigger the conformational changes that lead to release of phosphate and the formation of a strong actin–myosin interface undoubtedly involve a flexible loop that connects the upper and lower 50-kDa subdomains, and is commonly referred to as loop 2 (refs 24, 25). This loop does not contribute any interactions to our new structure, and thus is disordered. Binding to actin probably orders this loop and in doing so destabilizes the myosin–ADP–Pi structure and initiates cleft closure at the actin interface. Indeed, mutations in this loop can greatly slow and even prevent the release of phosphate and formation of strong actin binding in myosin II²⁵.

After phosphate release, myosin V populates a strong actin-binding state, with MgADP bound strongly to the nucleotide-binding site⁶. (This is the predominate steady-state intermediate of myosin V's actin-activated ATPase cycle⁶.) Clearly the alterations in the positions of the switch elements, P loop and β -sheet elements described above cannot occur and maintain tight binding of MgADP, as occurs for myosin V⁶ and other myosin isoforms⁹. Thus another state must exist in which there are changes in the relative positions of the upper and lower 50-kDa subdomains to achieve a high-affinity actin interface without significantly perturbing nucleotide binding.

We assert that myosin V populates a rigor-like conformation in the absence of both actin and nucleotide. This structure, in revealing the nature of the structural communication between the actin- and nucleotide-binding sites, provides an explanation of how strong binding of myosin to actin weakens the affinity of myosin for nucleotide, and vice versa. The major predictions of changes in the myosin structure that must occur for formation of the rigor complex with actin have been realized in this myosin V structure. It is important to note that myosin V is not an anomaly among myosins, as we also have a near-rigor state structure of this same myosin V construct in the presence of MgADP–BeFx (data not shown). Thus it is likely that the conformation we report here is essentially the same for all myosins when bound to actin in the absence of nucleotide, with the exception of the flexible loops at the actin interface that probably become ordered when myosin binds to actin. We refer to this new structural state of myosin as the closed-cleft state. □

Methods

Protein engineering and preparation

Myosin V was expressed using the baculovirus/SF9 cell expression system. The expression and purification were as previously described⁶. To create the recombinant virus used for expression, the complementary DNA coding for chicken myosin V was truncated after the codon corresponding to Arg 792. This construct encompassed the motor domain and the first light-chain/calmodulin-binding site of myosin V. A truncated cDNA for the LC1-sa light chain¹⁵ was co-expressed with the truncated myosin V heavy chain.

Crystallization, X-ray data collection and processing

Crystals were grown in hanging drops by vapour diffusion using equal amounts of reservoir solution (containing 6% PEG 8000, 50 mM MOPS pH 6.5, 2 mM DTT and 2 mM Na₃) and stock solution of the protein at 8 mg ml⁻¹. The protein/precipitant drops were microseeded the next day by streak seeding from previous crystallizations. The crystals belonged to the P2₁ space group (cell dimension: $a = 53.9 \text{ \AA}$, $b = 98.2 \text{ \AA}$, $c = 111.4 \text{ \AA}$ and $\beta = 101.4^\circ$, one molecule per asymmetric unit). An X-ray data set was collected up to 2 \AA at 100 K at the European Synchrotron Radiation Facility (ESRF) beamline ID-29 ($R_{\text{merge}} = 6.0\%$ (last shell = 33.5%)) with overall completeness 96.8% (2.12–2.05 \AA , 88.4%). We processed data using the programs DENZO²⁶ and SCALEPACK²⁶.

Structure refinement

The structure was solved by molecular replacement using the program AmoRe²⁷. The initial model was the motor domain of skeletal striated muscle (Protein Data Bank code 2MYS). Several steps of rigid body fitting performed with AmoRe²⁷ (each subdomain has been considered as a rigid group) were necessary to obtain a solution. We carried out model building and refinement using the program O²⁸ and Refmac5 (ref. 27). The final structure was refined to 2.0 \AA (R_{free} value, 26.3%; R_{cryst} value, 21.9%) and validated using the program PROCHECK²⁹. The main-chain dihedral angles for 92% of the non-glycine residues are in the maximum allowed region and none are in the disallowed region of the Ramachandran map. The model has root-mean-square deviations in bond length and bond angles of 0.014 \AA and 1.296°, respectively. Diagrams were computed using

MOLSCRIPT³⁰ and with the *Dictyostelium* myosin II structures (Protein Data Bank codes 1FMW and 1VOM). For Fig. 3, docking of myosin V was performed using a cryo-electron microscopy map of myosin II (K. C. Holmes and R. R. Schröder, personal communication and data not shown).

Received 13 March; accepted 18 July 2003; doi:10.1038/nature01927.

1. Holmes, K. C. & Geeves, M. A. Structural mechanism of muscle contraction. *Annu. Rev. Biochem.* **68**, 687–728 (1999).
2. Houdusse, A. & Sweeney, H. L. Myosin motors: missing structures and hidden springs. *Curr. Opin. Struct. Biol.* **11**, 182–194 (2001).
3. Mehta, A. D. E. *et al.* Myosin V is a processive actin-based motor. *Nature* **400**, 590–593 (1999).
4. Purcell, T. J., Morris, C., Spudich, J. A. & Sweeney, H. L. Role of the lever arm in the processive stepping of myosin V. *Proc. Natl Acad. Sci. USA* **99**, 14159–14164 (2002).
5. Titus, M. A. Myosin V—the multi-purpose transport motor. *Curr. Biol.* **7**, R301–R304 (1997).
6. De La Cruz, E. M., Wells, A. L., Safer, D., Ostap, E. M. & Sweeney, H. L. The kinetic mechanism of myosin V. *Proc. Natl Acad. Sci. USA* **96**, 13726–13731 (1999).
7. Dominguez, R., Freyzon, Y., Trybus, K. M. & Cohen, C. Crystal structure of a vertebrate smooth muscle myosin motor domain and its complex with the essential light chain: visualization of the pre-power stroke state. *Cell* **94**, 559–571 (1998).
8. Houdusse, A., Kalabokis, V. N., Himmel, D., Szent-Gyorgyi, A. G. & Cohen, C. Atomic structure of scallop myosin subfragment S1 complexed with MgADP: a novel conformation of the myosin head. *Cell* **97**, 459–470 (1999).
9. Whittaker, M. *et al.* A 35 Å movement of smooth muscle myosin on ADP release. *Nature* **378**, 748–751 (1995).
10. Fisher, A. J. *et al.* X-ray structures of the myosin motor domain of *Dictyostelium discoideum* complexed with MgADP·BeF₃⁻ and MgADP·AlF₄⁻. *Biochemistry* **34**, 8960–8972 (1995).
11. Kollmar, M., Durrwang, U., Kliche, W., Manstein, D. J. & Kull, F. J. Crystal structure of the motor domain of a class-I myosin. *EMBO J.* **21**, 2517–2525 (2002).
12. Rayment, I. *et al.* Three-dimensional structure of myosin subfragment-1: A molecular motor. *Science* **261**, 50–58 (1993).
13. Bauer, C. B., Holden, H. M., Thoden, J. B., Smith, R. & Rayment, I. X-ray structures of the apo and MgATP-bound states of *Dictyostelium discoideum* myosin motor domain. *J. Biol. Chem.* **275**, 38494–38499 (2000).
14. Coates, J. H., Criddle, A. H. & Geeves, M. A. Pressure-relaxation studies of pyrene-labelled actin and myosin subfragment-1 from rabbit skeletal muscle. *Biochem. J.* **232**, 351–356 (1985).
15. De La Cruz, E. M., Wells, A. L., Sweeney, H. L. & Ostap, E. M. Actin and light chain isoform dependence of myosin V kinetics. *Biochemistry* **39**, 14196–14202 (2000).
16. Taylor, E. W. Kinetic studies on the association and dissociation of myosin subfragment 1 and actin. *J. Biol. Chem.* **266**, 294–302 (1991).
17. Sasaki, N., Ohkura, R. & Sutoh, K. Insertion or deletion of a single residue in the strut sequence of *Dictyostelium* myosin II abolishes strong binding to actin. *J. Biol. Chem.* **275**, 38705–38709 (2000).
18. Rayment, I. *et al.* Structure of the actin-myosin complex and its implications for muscle contraction. *Science* **261**, 58–61 (1993).
19. Volkman, N. *et al.* Evidence for cleft closure in actomyosin upon ADP release. *Nature Struct. Biol.* **7**, 1147–1155 (2000).
20. Yengo, C. M., De La Cruz, E. M., Chrin, L. R., Gaffney, D. P. II & Berger, C. L. Actin-induced closure of the actin-binding cleft of smooth muscle myosin. *J. Biol. Chem.* **277**, 24114–24119 (2002).
21. Pasqualato, S., Renault, L. & Cherfils, J. Arf, Arp and Sar proteins: a family of GTP-binding proteins with a structural device for ‘front-back’ communication. *EMBO Rep.* **3**, 1035–1041 (2002).
22. Sasaki, N., Asukagawa, H., Yasuda, R., Hiratsuka, T. & Sutoh, K. Deletion of the myopathy loop of *Dictyostelium* myosin II and its impact on motor functions. *J. Biol. Chem.* **274**, 37840–37844 (1999).
23. Yengo, C. M., De La Cruz, E. M., Safer, D., Ostap, E. M. & Sweeney, H. L. Kinetic characterization of the weak binding states of myosin V. *Biochemistry* **41**, 8508–8517 (2002).
24. Spudich, J. A. How molecular motors work. *Nature* **372**, 515–518 (1994).
25. Joel, P. B., Trybus, K. M. & Sweeney, H. L. Two conserved lysines at the 50/20-kDa junction of myosin are necessary for triggering actin activation. *J. Biol. Chem.* **276**, 2998–3003 (2001).
26. Otwinowski, Z. & Minor, W. Processing of X-ray diffraction data collected in oscillation mode. *Methods Enzymol.* **276**, 307–325 (1997).
27. Collaborative Computational Project No. 4. The CCP4 suite: programs for protein crystallography. *Acta Crystallogr. D* **50**, 760–763 (1994).
28. Jones, T. A., Zou, J.-Y., Cowan, S. W. & Kjeldgaard, M. Improved methods for binding protein models in electron density maps and the location of errors in these models. *Acta Crystallogr. A* **47**, 110–119 (1991).
29. Laskowski, R. A., MacArthur, M. W., Moss, D. S. & Thornton, J. M. PROCHECK: a program to check the stereochemistry of protein structures. *J. Appl. Crystallogr.* **26**, 283–291 (1993).
30. Kraulis, P. J. MOLSCRIPT: a program to produce both detailed and schematic plots of protein structures. *J. Appl. Crystallogr.* **24**, 946–950 (1991).

Supplementary Information accompanies the paper on www.nature.com/nature.

Acknowledgements This work was supported by grants from the National Institutes of Health (H.L.S.), the CNRS and the ARC (A.H.). We thank D. Picot and the staff of the European Synchrotron Radiation Facility for assistance during data collection. We are also grateful to C. Baldacchino and J. Kibbe for help in protein purification.

Competing interests statement The authors declare that they have no competing financial interests.

Correspondence and requests for materials should be addressed to A.H. (anne.houdusse@curie.fr) or H.L.S. (lswsweeney@mail.med.upenn.edu). Atomic coordinates have been deposited in the Protein Data Bank under the accession code 1OE9.

Electron cryo-microscopy shows how strong binding of myosin to actin releases nucleotide

Kenneth C. Holmes, Isabel Angert, F. Jon Kull*, Werner Jahn & Rasmus R. Schröder

Department of Biophysics, Max Planck Institute for Medical Research, 69120 Heidelberg, Germany

* Present address: Dartmouth College, Hanover, New Hampshire 03755, USA

Muscle contraction involves the cyclic interaction of the myosin cross-bridges with the actin filament, which is coupled to steps in the hydrolysis of ATP¹. While bound to actin each cross-bridge undergoes a conformational change, often referred to as the “power stroke”², which moves the actin filament past the myosin filaments; this is associated with the release of the products of ATP hydrolysis and a stronger binding of myosin to actin. The association of a new ATP molecule weakens the binding again, and the attached cross-bridge rapidly dissociates from actin. The nucleotide is then hydrolysed, the conformational change reverses, and the myosin cross-bridge reattaches to actin. X-ray crystallography has determined the structural basis of the power stroke, but it is still not clear why the binding of actin weakens that of the nucleotide and vice versa. Here we describe, by fitting atomic models of actin and the myosin cross-bridge into high-resolution electron cryo-microscopy three-dimensional reconstructions, the molecular basis of this linkage. The closing of the actin-binding cleft when actin binds is structurally coupled to the opening of the nucleotide-binding pocket.

A complex of actin and myosin cross-bridges, formed by mixing fibres of actin with myosin cross-bridges in the absence of ATP (decorated actin), is a model system for the strong binding or ‘rigor’ state. Decorated actin has been studied by electron cryo-microscopy^{3–5}. To obtain higher resolution structural data, we have studied the actin–myosin cross-bridge complex by electron cryo-microscopy with ‘energy-filtering’. We have also used a new system for three-dimensional (3D) reconstruction to extract the maximum possible resolution from the data. Zero-loss energy-filtered imaging markedly improves the signal-to-noise ratio in the micrographs; in turn, this allows an accurate correction for the contrast transfer function and better alignment procedures during image processing, and thus a much improved resolution (14 Å) and a more detailed description of the actin–myosin interaction.

The structure of subfragment 1 (S1) of chicken skeletal myosin without bound nucleotide has been solved by X-ray crystallography⁶. It is a P-loop protein with switch 1 and switch 2 elements that are similar to those of the G proteins. The ATP is bound by the P-loop between the switch 1 and switch 2 elements. In the pre-power stroke state^{7,8}, both switch 1 and switch 2 make specific hydrogen-bond-mediated contact with the polyphosphate moiety of the ATP, particularly with the γ -phosphate. In the rigor state, the switch 2 element swings away.

Here, the actin filament structure was derived by fitting the crystal structure of monomeric actin (G-actin) to X-ray fibre diffraction patterns obtained from orientated gels of actin fibres (F-actin; see Supplementary Information).

The improvement in signal-to-noise ratio arising from using the energy filter allowed us to take data close to focus and at a relatively low electron dose (Fig. 1). By merging focal series at four different degrees of underfocus after correcting for the contrast transfer function⁹, we obtained the density shown as a surface representation in Fig. 2. The resolution of the map was 14 Å (for the resolution